ARTHRITIS & RHEUMATISM
Vol. 63, No. 5, May 2011, pp 1405–1415
DOI 10.1002/art.30262

Amelioration of Dermal Fibrosis by Genetic Deletion or Pharmacologic Antagonism of Lysophosphatidic Acid Receptor 1 in a Mouse Model of Scleroderma

Flavia V. Castelino,[1] Jon Seiders,[2] Gretchen Bain,[2] Sarah F. Brooks,[1] Christopher D. King,[2] James S. Swaney,[2] Daniel S. Lorrain,[2] Jerold Chun,[3] Andrew D. Luster,[1] and Andrew M. Tager[1]

Objective. **Scleroderma (systemic sclerosis [SSc]), is characterized by progressive multiorgan fibrosis. We recently implicated lysophosphatidic acid (LPA) in the pathogenesis of pulmonary fibrosis. The purpose of the present study was to investigate the roles of LPA and two of its receptors, LPA_1 and LPA_2, in dermal fibrosis in a mouse model of SSc.**

Methods. **Wild type (WT), and LPA_1-knockout (KO) and LPA_2-KO mice were injected subcutaneously with bleomycin or phosphate buffered saline (PBS) once daily for 28 days. Dermal thickness, collagen content, and numbers of cells positive for α-smooth muscle actin (α-SMA) or phospho-Smad2 were determined in bleomycin-injected and PBS-injected skin. In separate experiments, a novel selective LPA_1 antagonist AM095 or vehicle alone was administered by oral gavage to C57BL/6 mice that were challenged with 28 daily injections of bleomycin or PBS. AM095 or vehicle treatments were initiated concurrently with, or 7 or 14 days after, the initiation of bleomycin and PBS injections and continued to the end of the experiments. Dermal thickness and collagen content were determined in injected skin.**

Results. **The LPA_1-KO mice were markedly resistant to bleomycin-induced increases in dermal thickness and collagen content, whereas the LPA_2-KO mice were as susceptible as the WT mice. Bleomycin-induced increases in dermal α-SMA+ and phospho-Smad2+ cells were abrogated in LPA_1-KO mice. Pharmacologic antagonism of LPA_1 with AM095 significantly attenuated bleomycin-induced dermal fibrosis when administered according to either a preventive regimen or two therapeutic regimens.**

Conclusion. **These results suggest that LPA/LPA_1 pathway inhibition has the potential to be an effective new therapeutic strategy for SSc, and that LPA_1 is an attractive pharmacologic target in dermal fibrosis.**

Scleroderma (systemic sclerosis [SSc]), is a potentially fatal autoimmune disease of unknown cause, characterized by progressive multiorgan fibrosis that is refractory to current therapies. Fibrogenesis in SSc is thought to result from tissue injury, followed by dysregulated wound healing (1). Discovery of the mediators that drive aberrant wound healing responses will hopefully

Supported by an American College of Rheumatology Research and Education Foundation Physician Scientist Development Award to Dr. Castelino, by NIH grants R01-DA-019674, R01-NS-048478, and R01-DC-009505 to Dr. Chun, T32-AR-007258-32 to Dr. Luster, and R01-HL-095732 to Dr. Tager, and by a Scleroderma Research Foundation grant to Dr. Tager.

[1]Flavia V. Castelino, MD, Sarah F. Brooks, BSc, Andrew D. Luster, MD, PhD, Andrew M. Tager, MD: Massachusetts General Hospital and Harvard Medical School, Boston, Massachusetts; [2]Jon Seiders, PhD, Gretchen Bain, PhD, Christopher D. King, PhD, James S. Swaney, PhD, Daniel S. Lorrain, PhD: Amira Pharmaceuticals, San Diego, California; [3]Jerold Chun, MD, PhD: The Scripps Research Institute, La Jolla, California.

Drs. Seiders, Bain, King, Swaney, Lorrain, and Chun own stock or stock options in Amira Pharmaceuticals. Drs. Chun and Tager have received consulting fees and/or honoraria from Amira Pharmaceuticals (less than $10,000 each) and serve as members of the company's Scientific Advisory Board. Drs. Luster and Tager have filed a patent cooperation treaty application on lysophosphatidic acid receptor targeting in lung disease.

Address correspondence to Andrew M. Tager, MD, Center for Immunology and Inflammatory Diseases, Massachusetts General Hospital, 149 13th Street, Room 8301, Charlestown, MA 02129. E-mail: amtager@partners.org.

Submitted for publication August 13, 2010; accepted in revised form January 18, 2011.

identify new therapeutic targets for SSc. We hypothesize that one such target is LPA_1, a receptor for lysophosphatidic acid (LPA).

LPA is a lipid mediator that signals through specific G protein–coupled receptors. Five high-affinity LPA receptors have been definitively established and designated LPA_1 to LPA_5; $P2Y_5$ is a lower affinity receptor that is likely to join the LPA receptor family as LPA_6 (2). Our laboratory recently implicated LPA/LPA_1 signaling in the pathogenesis of pulmonary fibrosis (3). We found that LPA_1-knockout (KO) mice were dramatically protected from bleomycin-induced pulmonary fibrosis and mortality and that LPA/LPA_1 signaling was responsible for the majority of fibroblast chemoattractant activity present in bronchoalveolar lavage fluid from patients with idiopathic pulmonary fibrosis. LPA/LPA_2 signaling has also been implicated in pulmonary fibrosis. LPA/LPA_2 signaling can induce $\alpha v\beta 6$ integrin-mediated activation of latent transforming growth factor β (TGFβ) by lung epithelial cells in culture (4), and TGFβ activation by this integrin is critically required for the development of bleomycin-induced lung fibrosis (5).

LPA may also be involved in the pathogenesis of SSc, as suggested by the recent demonstration that arachidonoyl (20:4) LPA levels are significantly higher in SSc patients' serum versus healthy controls (6). Injured human skin has been shown to contain increased amounts of both LPA and cells expressing LPA_1 (7). We therefore investigated whether LPA signaling through either LPA_1 or LPA_2 is required for dermal fibrosis in the bleomycin model of scleroderma. In this model, repeated subcutaneous injections of the chemotherapeutic agent bleomycin results in dermal fibrosis that resembles scleroderma (8), with collagen deposition and both fibroblast and myofibroblast accumulation (9). Lesional skin also shows increased Smad2 and Smad3 phosphorylation (10), indicating activation of the TGFβ pathway, which is implicated in scleroderma (11,12). We found that bleomycin-induced increases in dermal thickness, collagen content, myofibroblast accumulation, and Smad2 phosphorylation were all markedly attenuated in LPA_1-KO mice. Bleomycin-induced dermal fibrosis was also significantly reduced in wild-type (WT) mice treated with the novel, orally bioavailable, LPA_1-selective antagonist AM095. In contrast, LPA_2-KO mice were not protected from bleomycin-induced dermal fibrosis. These results indicate that LPA/LPA_1 signaling contributes importantly to injury-induced dermal fibrosis.

MATERIALS AND METHODS

Animals. Experiments comparing LPA_1-KO and WT mice used offspring of mice heterozygous for the LPA_1 mutant allele, which were hybrids of the C57BL/6 and 129Sv/J genetic backgrounds (13). LPA_1-KO mice (generated in Dr. Jerold Chun's Laboratory at The Scripps Research Institute) demonstrate impaired suckling in neonatal pups because of defective olfaction, which leads to increased neonatal death and reduced body size in survivors. Survivors also demonstrate craniofacial dysmorphism characterized by shorter snouts and more widely spaced eyes (13), but we have not noted any skin abnormalities at baseline.

Experiments comparing LPA_2-KO and WT mice used offspring of mice homozygous for the mutant LPA_2 allele in the BALB/c genetic background (14) and WT BALB/c mice (Charles River Laboratories). LPA_2-KO mice (also generated in Dr. Chun's Laboratory) are born at the expected frequency and display no obvious phenotype abnormalities (14).

Experiments measuring plasma AM095 concentrations and comparing AM095-treated and vehicle-treated mice used WT C57BL/6 mice from Harlan Laboratories and the National Cancer Institute-Frederick Mouse Repository, respectively.

All experiments used sex- and age-matched mice at 6–8 weeks of age that were maintained in specific pathogen–free environments. All experiments were performed in accordance with National Institute of Health guidelines and with protocols approved by the Massachusetts General Hospital or the Amira Pharmaceuticals Institutional Animal Care and Use Committee.

Bleomycin injections and skin harvests. Bleomycin (Gensia Sicor) was dissolved in phosphate buffered saline (PBS) at 10 μg/ml and sterilized by filtration. Bleomycin or PBS (100 μl) was injected subcutaneously into 2 locations on the shaved back of LPA_1-KO, LPA_2-KO, or WT mice, once daily for 28 days. Mice were then killed, and full-thickness 6-mm punch biopsies were obtained from each injection site. One skin sample was fixed in 10% formalin and embedded in paraffin for histologic and immunohistochemical studies; the other was immediately frozen at –80°C for hydroxyproline analysis.

Histologic analysis and dermal thickness measurement. Multiple 5-μm sections of paraffin-embedded skin samples were deparaffinized, rehydrated, and stained with hematoxylin and eosin (H&E) or with Masson's trichrome according to the standard protocols of our laboratory (3). Dermal thickness was determined with the use of photomicrographs (100× magnification) of H&E-stained sections, measuring the distance between the epidermal–dermal junction and the dermal–fat junction at 5 randomly selected sites per high-power field in 10 high-power fields per section.

Immunohistochemical analyses of α-smooth muscle actin (α-SMA) and phospho-Smad2. Multiple 5-μm sections of paraffin-embedded skin samples were cut onto ProbeOn Plus slides (Fisher Scientific), deparaffinized, and rehydrated. Immunolabeling of α-SMA and phospho-Smad2 was performed with primary rabbit anti-mouse α-SMA antibody (Abcam) and primary rabbit anti-mouse phospho-Smad2 antibody (Cell Signaling), respectively, using the MicroProbe staining system (Fisher Scientific) according to the manufacturer's instructions. Appropriate biotinylated secondary antibodies

were used, followed by detection with an avidin–biotin–peroxidase complex development kit (Vector) and color development with aminoethylcarbazole (Dako). Cells positive for α-SMA and for phospho-Smad2 were then counted in 10 randomly selected, nonoverlapping high-power fields in dermal sections from WT and LPA_1-KO mice.

Hydroxyproline assay. Hydroxyproline content as a measure of skin collagen was determined using the standard protocol of our laboratory (15). Briefly, skin samples were homogenized in PBS and hydrolyzed overnight in 6*N* HCl at 120°C. A 25-μl aliquot was desiccated, resuspended in 25 μl of H_2O, and added to 0.5 ml of 1.4% chloramine T (Sigma), 10% *n*-propranolol, and 0.5*M* sodium acetate, pH 6.0. After a 20-minute incubation at room temperature, 0.5 ml of Ehrlich's solution (1*M* *p*-dimethylaminobenzaldehyde [Sigma] in 70% *n*-propranolol, 20% perchloric acid) was added. After a 15-minute incubation at 65°C, absorbance was measured at 550 nm, and the hydroxyproline concentration was determined against a standard curve. Assay results were expressed as micrograms of hydroxyproline per 6-mm punch biopsy sample of skin.

Cell lines and culture. Human and mouse LPA_1 and human LPA_3 receptors were stably expressed in Chinese hamster ovary (CHO) cells (Invitrogen) and cultured in Ham's F-12 medium with 10% fetal bovine serum (FBS) and 1 mg/ml of hygromycin B. Mouse LPA_3 was stably expressed in human embryonic kidney (HEK) cells (Invitrogen) and cultured in Dulbecco's modified Eagle's medium with 10% FBS and 200 μg/ml of hygromycin B. Human and mouse LPA_2 and LPA_5 and human LPA_4 were transiently expressed in rat neuroblastoma B103 cells using Lipofectamine 2000 (Invitrogen) according to the manufacturer's instructions.

Calcium flux assay. LPA receptor–transfected cells were plated in 96-well poly-D-lysine–coated black-wall clear-bottomed plates (BD BioCoat) at 20,000–40,000 cells/well and cultured overnight in complete medium. Cells were then washed with PBS and cultured in serum-free medium either overnight (for stably expressing cells) or for 4 hours (for transient transfectants) prior to dye loading. On the day of the assay, cells were loaded for 1 hour at 37°C with 100 μl of FLIPR Calcium 4 dye (Molecular Devices) in Hanks' balanced salt solution (HBSS) supplemented with 20 m*M* HEPES, 2 m*M* probenecid, and 0.3% fatty acid–free human serum albumin. Test compounds (in 25 μl of 1% DMSO) were added to each well and incubated at room temperature for 30 minutes. LPA (50 μl of 5× stock solutions prepared in HBSS with 20 m*M* HEPES and 0.3% fatty acid–free human serum albumin) was added after 15 seconds of baseline measurement. The final concentrations of LPA used were dependent on the receptor expressed: LPA_1 and LPA_3 assays used 10 n*M* LPA, LPA_2 and LPA_5 assays used 30 n*M* LPA, and LPA_4 assay used 300 n*M* LPA. Intracellular calcium mobilization was measured using a FlexStation III (Molecular Devices). Inhibition curves were generated by plotting the percentage inhibition of calcium flux versus $\log_{10}$ of the concentration of compound. The 50% inhibition concentration (IC_{50}) was calculated by nonlinear regression using the sigmoidal dose-response (variable slope) equation in Prism 5 software (GraphPad Software).

Determination of AM095 concentrations in mouse plasma. C57BL/6 mice were administered the selective LPA_1 antagonist AM095 by oral gavage (30 mg/kg) at time 0 and at 8 hours, and blood was collected by cardiac puncture under anesthesia into tubes containing sodium EDTA at 0, 4, 8, 9, 12, and 24 hours. Plasma samples were stored at −40°C prior to analysis of AM095 concentrations by liquid chromatography tandem mass spectrometry. Known amounts of AM095 were added to thawed mouse plasma to yield a concentration range from 0.8 ng/ml to 4,000 ng/ml. Plasma samples were precipitated using acetonitrile containing the internal standard buspirone. The analyte mixture (10 μl) was injected using a Leap PAL autosampler. Calibration curves were constructed by plotting the peak area ratio of analyzed peaks against known concentrations. The lower limit of quantitation was 1 ng/ml. The data were examined by linear regression analysis with $1/\chi^2$ weighting. The pharmacokinetic parameters of AM095 were calculated by noncompartmental analysis using WinNonlin Professional software (Pharsight). The maximum concentration (C_{max}) and the time to maximum concentration (T_{max}) were obtained directly from the measured data.

AM095 administration in the bleomycin model. The selective LPA_1 antagonist AM095 was dissolved in sterile water, and a dose of 30 mg/kg of AM095 or sterile water alone (vehicle), was administered by oral gavage to each C57BL/6 mouse, twice daily on weekdays and once daily on weekends. AM095 was administered from the initiation of bleomycin challenge in a preventive regimen or beginning either 7 or 14 days after the initiation of bleomycin challenge in 2 therapeutic regimens. For all AM095 regimens, bleomycin or PBS was injected subcutaneously for 28 consecutive days, and skin samples were obtained at the completion of the experiment as described above.

Statistical analysis. Differences in dermal thickness, hydroxyproline content, and the numbers of α-SMA+ and phospho-Smad2+ cells between WT mice and LPA_1-KO or LPA_2-KO mice and between AM095-treated mice and vehicle-treated mice were tested for statistical significance by Student's 2-tailed *t*-test, using Microsoft Excel software. *P* values less than 0.05 were considered significant.

RESULTS

Dependence of bleomycin-induced dermal fibrosis on LPA_1. Examination of H&E-stained skin sections of bleomycin- and PBS-challenged WT and LPA_1-KO mice demonstrated that LPA_1-KO mice were strikingly protected from bleomycin-induced dermal fibrosis (Figure 1A, upper panels). Compared with PBS-challenged mice, bleomycin-challenged WT mice demonstrated substantial thickening of the dermis, with densely packed connective tissue replacing the subcutaneous fat. These changes were markedly reduced in bleomycin-challenged LPA_1-KO mice. The substantial increase in dermal collagen induced by bleomycin in WT mice was also markedly attenuated in LPA_1-KO mice, as demonstrated by Masson's trichrome staining (Figure 1A, lower panels).

To quantify the protection of LPA_1-KO mice against dermal fibrosis, we first assessed dermal thick-

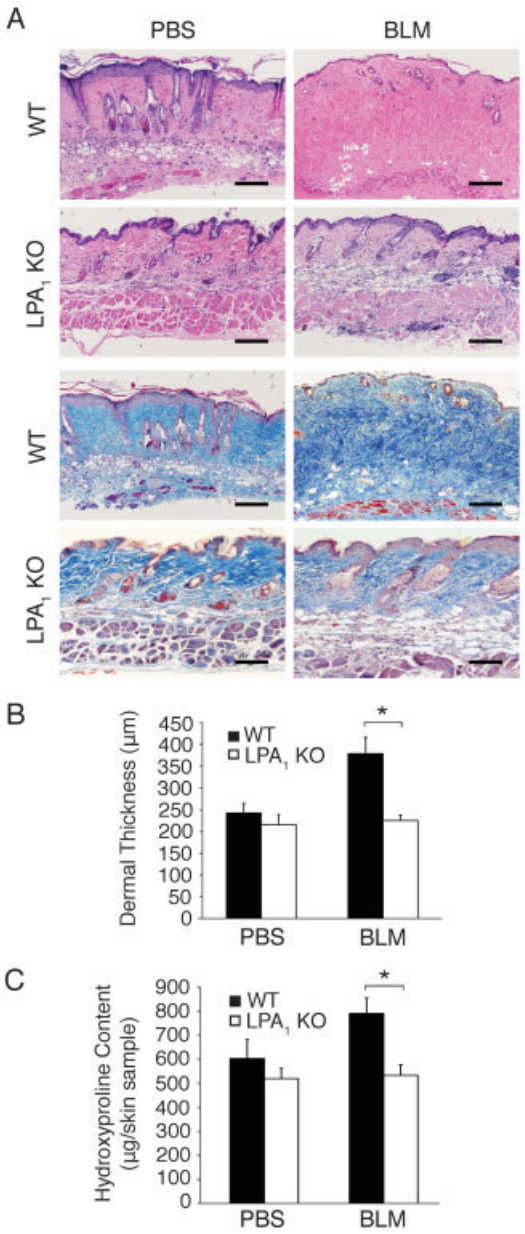

Figure 1. Protection of lysophosphatidic acid receptor 1 (LPA_1)–knockout (KO) mice from bleomycin (BLM)–induced dermal fibrosis. **A,** Skin sections from wild-type (WT) and LPA_1-KO mice following challenge with phosphate buffered saline (PBS) or BLM and staining with hematoxylin and eosin (upper panels) or with Masson's trichrome (lower panels). Bars = 100 μm. **B,** Dermal thickness, measured as the distance between the epidermal–dermal junction and the dermal–fat junction at 5 randomly selected sites per high-power field in 10 high-power fields per skin sample. $* = P < 0.001$ for BLM-challenged WT versus LPA_1-KO mice. Differences between BLM- and PBS-challenged WT mice were also significant ($P = 0.02$). **C,** Skin hydroxyproline content in a 6-mm punch biopsy skin sample. $* = P < 0.001$ for BLM-challenged WT versus LPA_1-KO mice. Differences between BLM- and PBS-challenged WT mice were also significant ($P < 0.01$). Data in **B** and **C** are from 1 of 2 independent experiments that yielded similar results. Values are the mean ± SEM of ≥5 mice per treatment group.

ness in bleomycin- and PBS-challenged WT and LPA_1-KO mice. The dermal thickness in bleomycin-challenged LPA_1-KO mice was significantly reduced compared with that in WT mice (Figure 1B). Whereas bleomycin challenge increased the dermal thickness in WT mice by 56%, the dermal thickness in bleomycin-challenged LPA_1-KO mice was only 5% greater than that in PBS-challenged LPA_1-KO mice (Figure 1B). Genetic deletion of LPA_1 therefore attenuated the increase in bleomycin-induced dermal thickness by 91%.

Biochemical assessment of skin collagen by measuring the hydroxyproline content confirmed the significant protection of LPA_1-KO mice. Bleomycin challenge increased the amount of skin hydroxyproline by 31% in WT mice, but only by 3% in LPA_1-KO mice (Figure 1C). Genetic deletion of LPA_1 therefore attenuated the bleomycin-induced increase in hydroxyproline by 90%. This dramatic protection of LPA_1-KO mice suggests that the LPA/LPA_1 pathway contributes importantly to dermal fibrosis.

No requirement for LPA_2 in bleomycin-induced dermal fibrosis. In contrast to the LPA_1-KO mice, the LPA_2-KO mice were not protected from bleomycin-induced dermal fibrosis. Bleomycin induced similar thickening of the dermis, with densely packed connective tissue, in LPA_2-KO mice as in WT mice and similar increases in dermal collagen, as demonstrated in skin sections stained with H&E (Figure 2A, upper panels) and Masson's trichrome (Figure 2A, lower panels), respectively. Dermal thickness and hydroxyproline content measurements confirmed that LPA_2 deletion did not confer protection from bleomycin-induced fibrosis. Compared to the findings in PBS-challenged mice, bleomycin challenge increased dermal thickness by 46% in WT mice and by 50% in LPA_2-KO mice (Figure 2B). Similarly, bleomycin increased the skin hydroxyproline content by 67% in WT mice and by 66% in LPA_2-KO mice (Figure 2C). The lack of protection of LPA_2-KO mice by bleomycin suggests that LPA_2 signaling is not required for dermal fibrosis.

Dependence of bleomycin-induced dermal myofibroblast accumulation on LPA_1. To begin to investigate the mechanism(s) through which LPA and LPA_1 contribute to dermal fibrosis, we assessed two processes implicated in scleroderma, accumulation of myofibroblasts and activation of the TGFβ/Smad signaling pathway, in bleomycin-challenged WT and LPA_1-KO mice. SSc fibrogenesis is associated with fibroblast differentiation into myofibroblasts, which secrete increased amounts of extracellular matrix components, including

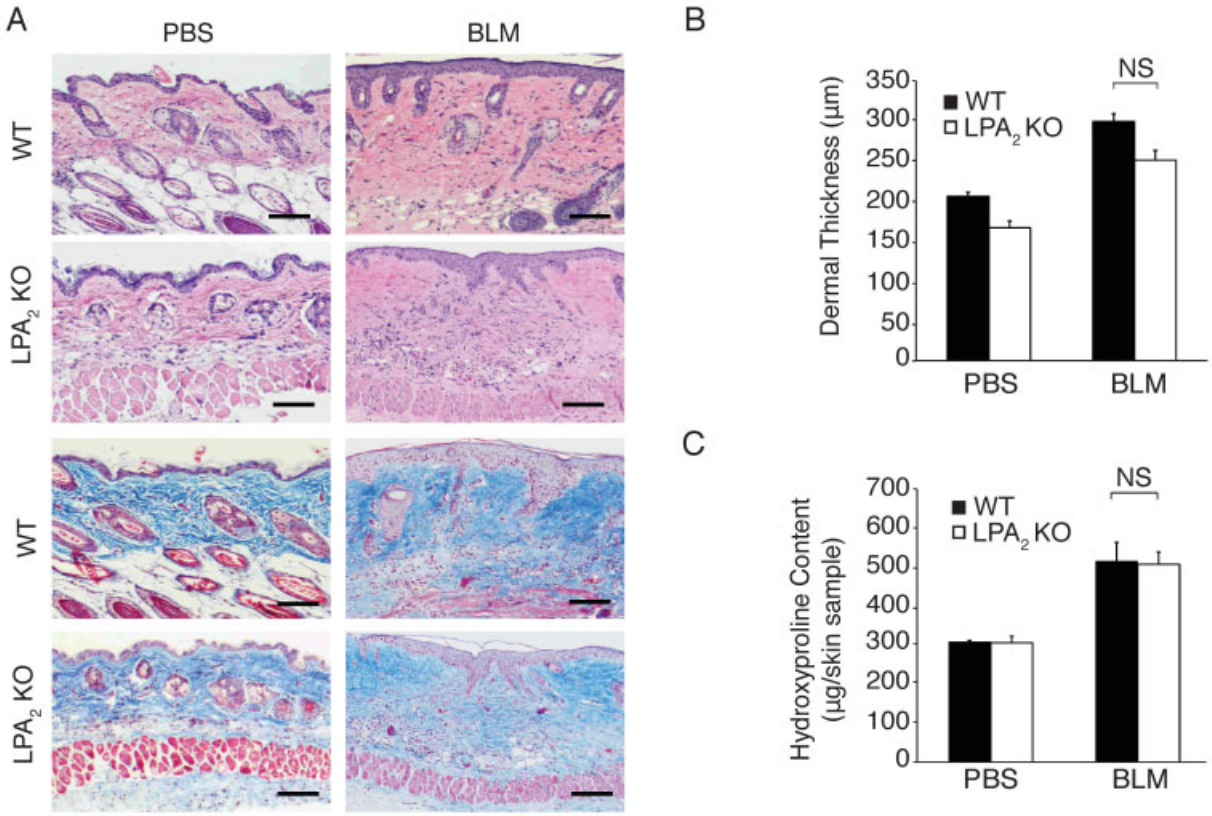

Figure 2. Lack of protection of LPA_2-KO mice from BLM-induced dermal fibrosis. **A,** Skin sections from WT and LPA_2-KO mice following challenge with PBS or BLM and staining with hematoxylin and eosin (upper panels) or with Masson's trichrome (lower panels). Bars = 100 μm. **B,** Dermal thickness, measured as the distance between the epidermal–dermal junction and the dermal–fat junction at 5 randomly selected sites per high-power field in 10 high-power fields per skin sample. Differences were significant between BLM-challenged and PBS-challenged WT mice ($P < 0.002$) and between BLM-challenged and PBS-challenged LPA_2-KO mice ($P < 0.001$). The difference between BLM-challenged WT mice and BLM-challenged LPA_2-KO mice was not significant (NS). **C,** Skin hydroxyproline content in a 6-mm punch biopsy skin sample. Differences were significant between BLM-challenged and PBS-challenged WT mice ($P < 0.003$) and between BLM-challenged and PBS-challenged LPA_2-KO mice ($P < 0.002$). The difference between BLM-challenged WT mice and BLM-challenged LPA_2-KO mice was not significant. Data in **B** and **C** are from 1 of 2 independent experiments that yielded similar results. Values are the mean ± SEM of ≥5 mice per treatment group. See Figure 1 for other definitions.

collagen (16). Myofibroblast differentiation is characterized by the acquisition of smooth muscle cell features, including α-SMA expression (17).

To determine whether LPA/LPA_1 signaling contributes to bleomycin-induced myofibroblast accumulation, we compared the number of α-SMA+ cells in the dermis of bleomycin- and PBS-challenged WT and LPA_1-KO mice. Bleomycin challenge substantially increased the number of α-SMA+ cells in the dermis of WT mice but not LPA_1-KO mice (Figure 3A). The number of α-SMA+ cells increased by 70% in bleomycin-challenged WT mice, but only by 5% in LPA_1-KO mice (Figure 3B), suggesting that LPA and LPA_1 make important contributions to myofibroblast accumulation in dermal fibrosis.

Dependence of bleomycin-induced dermal Smad2 phosphorylation on LPA_1. Myofibroblast differentiation and synthesis of matrix proteins are driven by TGFβ (18,19). By directing these key profibrotic processes, TGFβ is thought to play a central role in SSc fibrogenesis. When bound by active TGFβ, TGFβ receptors transmit signals through phosphorylation of cytoplasmic Smad proteins, which translocate to the nucleus and act as transcription factors (20). To determine whether LPA/LPA_1 signaling contributes to the activation of the TGFβ signaling pathway following bleomycin challenge, we compared the number of cells with nuclear Smad2 phosphorylation in the dermis of bleomycin- and PBS-challenged WT and LPA_1-KO mice.

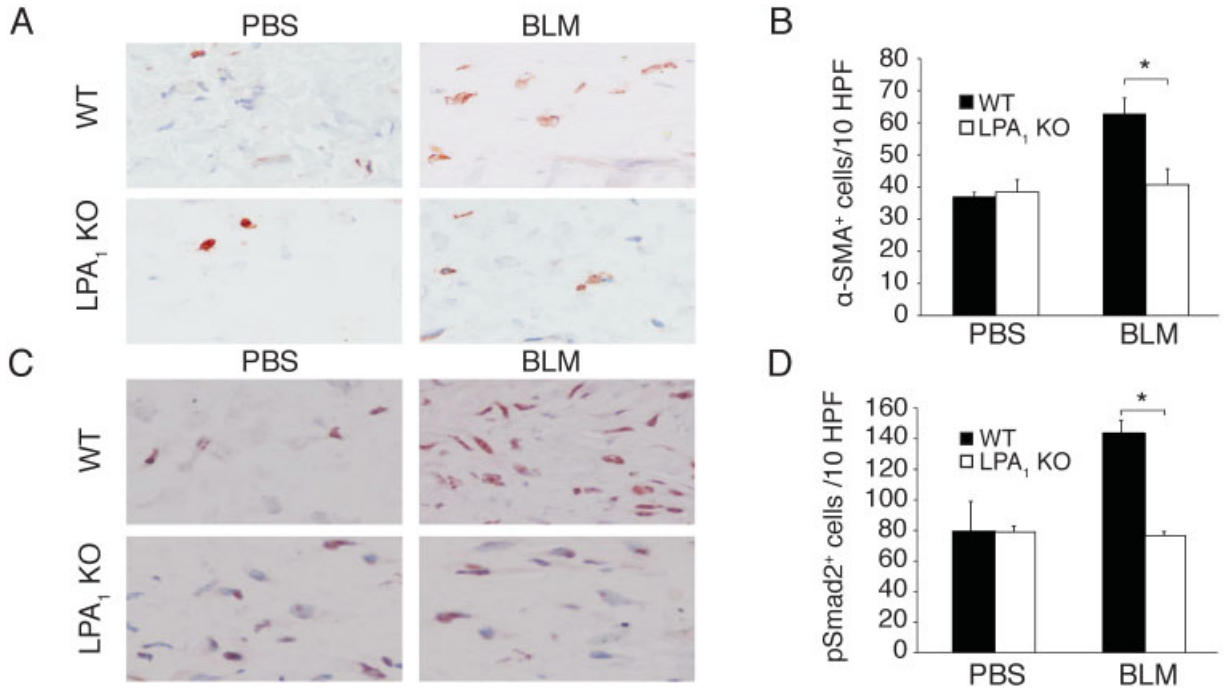

Figure 3. Diminished accumulation of α-smooth muscle actin (α-SMA)–positive myofibroblasts and phospho-Smad2+ cells in BLM-challenged LPA_1-KO mice. **A,** Skin sections from WT and LPA_1-KO mice following challenge with PBS or BLM and staining with anti–α-SMA antibody. Original magnification × 400. **B,** Quantification of α-SMA+ cells in the dermis of WT and LPA_1-KO mice following challenge with PBS or BLM. * = $P < 0.01$ for BLM-challenged WT versus LPA_1-KO mice. Differences between BLM- and PBS-challenged WT mice were also significant ($P < 0.001$). The difference between BLM-challenged and PBS-challenged LPA_1-KO mice was not significant. **C,** Skin sections from WT and LPA_1-KO mice following challenge with PBS or BLM and staining with anti–phospho-Smad2 antibody. Original magnification × 400. **D,** Quantification of pSmad2+ cells in the dermis of WT and LPA_1-KO mice following challenge with PBS or BLM. * = $P < 0.002$ for BLM-challenged WT versus LPA_1-KO mice. Differences between BLM- and PBS-challenged WT mice were also significant ($P < 0.03$). The difference between BLM-challenged and PBS-challenged LPA_1-KO mice was not significant. Data in **B** and **D** are from 1 of 2 independent experiments that yielded similar results. Values are the mean ± SEM of 10 high-power fields in sections from 6 mice per treatment group for α-SMA studies and from 3 mice per treatment group for phospho-Smad2 studies. See Figure 1 for other definitions.

Bleomycin challenge increased the number of nuclear phospho-Smad2+ cells in the dermis of WT mice but not LPA_1-KO mice (Figure 3C). The number of phospho-Smad2+ cells increased by 81% in bleomycin-challenged WT mice, but did not increase at all in LPA_1-KO mice (Figure 3D), suggesting that LPA and LPA_1 may contribute to the activation of the TGFβ/Smad signaling pathway during the development of dermal fibrosis. Alternatively, the reduced number of nuclear phospho-Smad2+ cells in bleomycin-challenged LPA_1-KO mice could be at least partly attributable to reductions in the numbers of fibroblasts and myofibroblasts accumulating in the dermis of these mice. Reductions in fibroblast and myofibroblast numbers would reduce the number of cells present in the dermis that are able to respond to TGFβ by Smad phosphorylation.

Potent and selective LPA_1 antagonism by AM095. To investigate the potential of LPA_1 as a therapeutic agent for dermal fibrosis, we evaluated a potent new LPA_1-selective antagonist, AM095 (sodium{4′-[3-methyl-4-((*R*)-1-phenyl-ethoxycarbonylamino)-isoxazol-5-yl]-biphenyl-4-yl}-acetate) (Figure 4A). AM095 inhibited the LPA-induced calcium flux of CHO cells that had been stably transfected with human or mouse LPA_1 (Figure 4B). The IC_{50} for AM095 antagonism of LPA-induced calcium flux of human or mouse LPA_1-transfected CHO cells was 0.025 μM and 0.023 μM, respectively (Table 1). In contrast, the IC_{50} for AM095 antagonism of LPA-induced calcium flux was >5 μM for CHO cells, HEK cells, or B103 cells transfected with 1 of the other 4 established human or mouse LPA receptors, demonstrating the selectivity of AM095 for LPA_1 (Table 1).

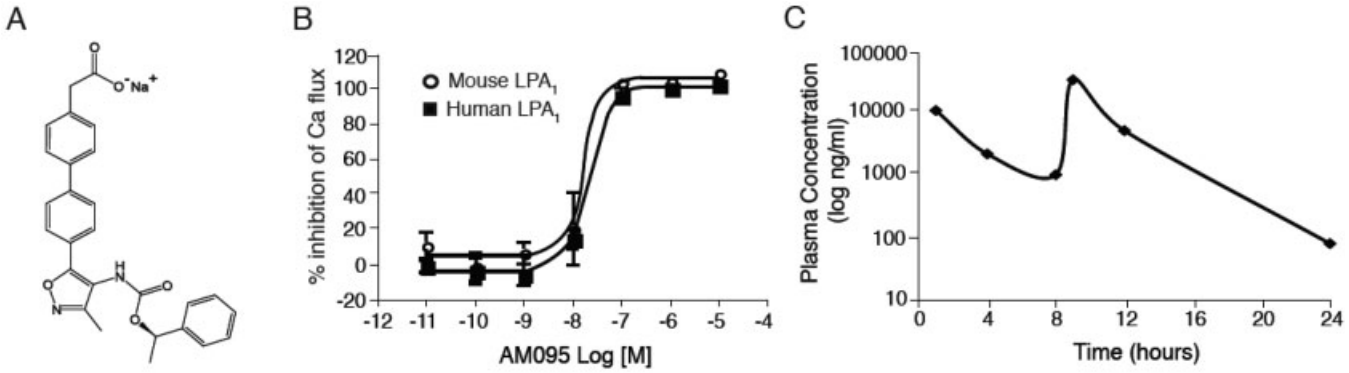

Figure 4. Structure and pharmacokinetics of AM095. **A,** Chemical structure of the selective lysophosphatidic acid receptor 1 (LPA_1) antagonist, AM095 (sodium{4′-[3-methyl-4-((*R*)-1-phenyl-ethoxycarbonylamino)-isoxazol-5-yl]-biphenyl-4-yl}-acetate). **B,** AM095 inhibition of LPA-induced calcium flux in Chinese hamster ovary cells recombinantly expressing human or mouse LPA_1. Values are the mean ± SEM of 5 cultures for cells expressing human LPA_1 and 3 cultures for mouse LPA_1. **C,** Average plasma concentrations of AM095 at the indicated time points in C57BL/6 mice given 30 mg/kg of AM095 by oral gavage at 0 and 8 hours (n = 2 mice per time point analyzed).

The average plasma concentrations of AM095 produced in mice over a 24-hour period by the administration of two 30-mg/kg doses by oral gavage given 8 hours apart are shown in Figure 4C. The AM095 AUC value was 118.7 $\mu g \cdot$ hour/ml, with a plasma C_{max} of 6,200 n*M* (28 μg/ml) and a plasma C_{min} of 170 n*M* (0.08 μg/ml). Twice daily 30-mg/kg dosing by oral gavage was therefore used in all subsequent experiments, since this produced plasma AM095 concentrations that were greater than the IC_{50} for the LPA_1 receptor throughout the treatment period.

Attenuation of bleomycin-induced dermal fibrosis by preventive and therapeutic AM095 regimens. Administration of AM095 from the initiation of bleomycin challenge in a preventive regimen attenuated bleomycin-induced dermal fibrosis, substantially mitigating the bleomycin-induced increases in dermal thickness and dermal collagen, as demonstrated in skin sections stained with H&E (Figure 5A, left panels) and Masson's trichrome (Figure 5A, right panels) respectively.

Delayed administration of AM095 until after the initiation of bleomycin challenge was performed in two therapeutic regimens, one beginning on day 7 and the other beginning on day 14 after initiation of bleomycin challenge; these regimens also attenuated bleomycin-induced dermal fibrosis. Measurements of dermal thickness and hydroxyproline content indicated the protective efficacy of treatment according to all 3 regimens. Bleomycin challenge increased the dermal thickness of vehicle-treated mice by 82%, but by only 25%, 12%, and 32% for the preventive, therapeutic day 7, and therapeutic day 14 regimens, respectively, in AM095-treated mice (Figure 5B). Preventive pharmacologic inhibition of LPA_1 therefore attenuated the bleomycin-induced increase in dermal thickness by 70%, while therapeutic pharmacologic inhibition of LPA_1 begun on day 7 or on day 14 attenuated the bleomycin-induced increase in dermal thickness by 85% and 61%, respectively.

Similarly, bleomycin challenge increased the hydroxyproline content of skin from vehicle-treated mice by 117%, but by only 56%, 79%, or 86% for the preventive, therapeutic day 7, and therapeutic day 14 regimens, respectively, in AM095-treated mice (Figure 5C). Preventive inhibition of LPA_1 therefore attenuated the bleomycin-induced increase in hydroxyproline by 52%, while therapeutic inhibition of LPA_1 begun on day 7 or day 14 attenuated the bleomycin-induced increase in hydroxyproline by 32% and 26%, respectively. These data suggest an ongoing requirement for the LPA/LPA_1

Table 1. AM095 inhibition of LPA-stimulated intracellular calcium release from cells recombinantly expressing $LPA_{1–5}$*

	IC_{50}, μM	
	Human cells	Mouse cells
LPA_1	0.025 (5)	0.023 (3)
LPA_2	>10 (3)	>10 (3)
LPA_3	>10 (5)	5.4 (4)
LPA_4	8.5 (2)	ND
LPA_5	>10 (3)	>10 (3)

* Calcium release from lysophosphatidic acid (LPA)–stimulated human and mouse cells expressing individual LPA receptors 1–5 was determined as described in Materials and Methods. Values are the 50% inhibition concentration (IC_{50}). Numbers in parentheses are the number of cell cultures tested. ND = not done.

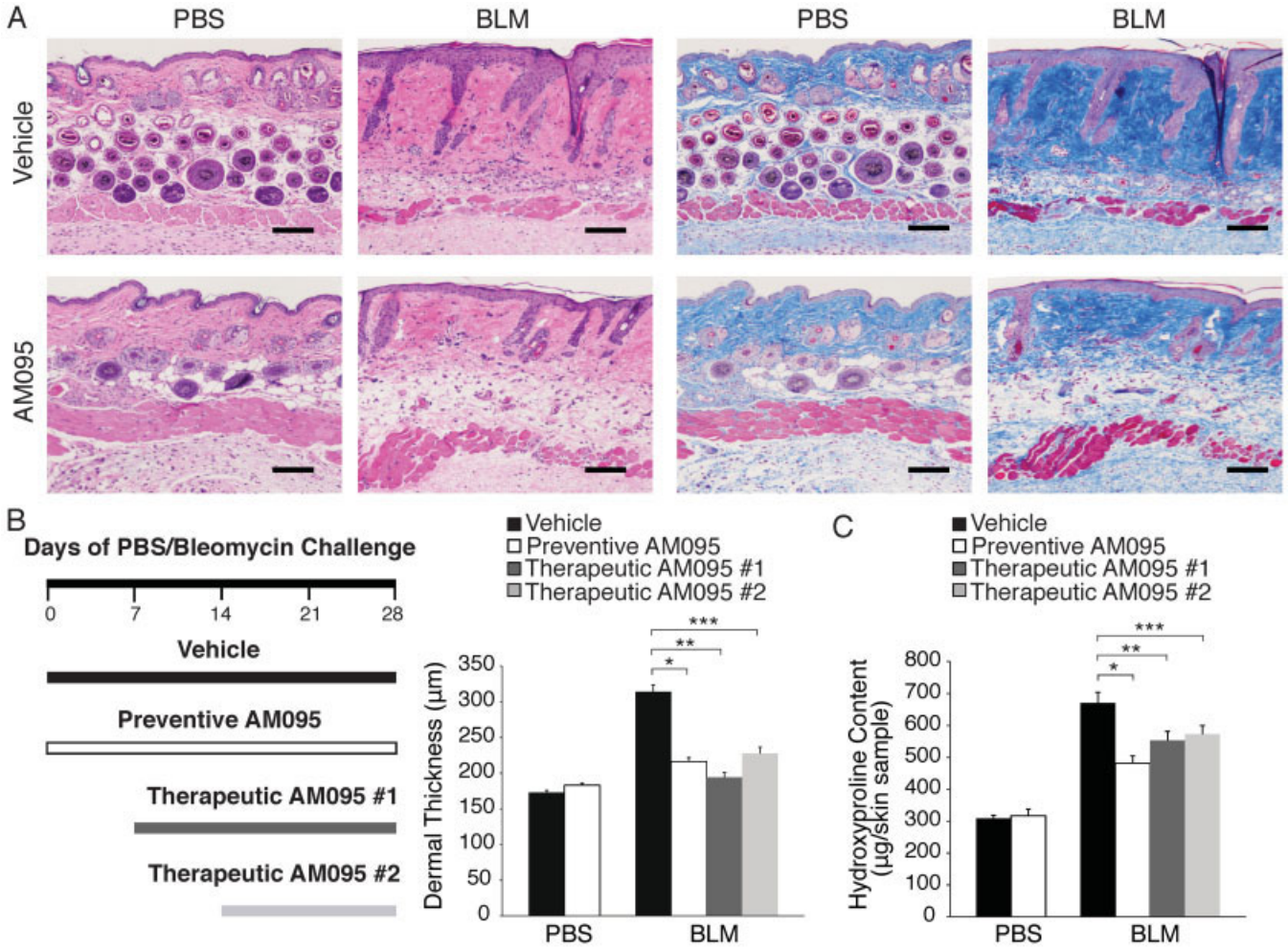

Figure 5. Attenuation of BLM-induced fibrosis by pharmacologic antagonism of lysophosphatidic acid receptor 1 (LPA_1). **A,** Skin sections from PBS- or BLM-challenged C57BL/6 mice treated with vehicle or with AM095 in a preventive regimen. Sections were stained with hematoxylin and eosin (left panels) and Masson's trichrome (right panels). Bars = 100 μm. **B,** Dermal thickness of PBS- or BLM-challenged C57BL/6 mice treated with vehicle, preventive AM095, or therapeutic AM095 begun on day 7 (AM095 #1) or on day 14 (AM095 #2) after challenge with PBS or BLM. $* = P < 0.0008$; $** = P < 0.002$; $*** = P < 0.01$. **C,** Skin hydroxyproline content in 6-mm punch biopsy skin samples obtained from the same mice as in **A**. $* = P < 0.0005$; $** = P < 0.02$; $*** = P < 0.02$. Values in **B** and **C** are the mean ± SEM of 3 mice per treatment group for the dermal thickness studies and of 5 mice per group for the hydroxyproline content studies. Data for the PBS-challenged, vehicle-treated BLM-challenged, and preventive AM095 BLM-challenged groups were combined from 2 experiments; data for both therapeutic AM095 BLM-challenged groups were from 1 experiment. See Figure 1 for other definitions.

pathway in the maintenance of pathologic dermal fibrosis, suggesting that this pathway is a viable target for therapeutic intervention in fibrotic diseases of the skin.

DISCUSSION

Our results demonstrate that LPA_1 is required for the development of bleomycin-induced dermal fibrosis. Genetic deletion of this receptor or pharmacologic antagonism with a new orally bioavailable selective inhibitor protected mice from the increases in dermal thickness and collagen content produced in this model. In contrast, genetic deletion of LPA_2 did not confer protection against dermal fibrosis. Taken together, these data suggest that LPA signaling specifically through LPA_1 is critical for the development of skin fibrosis induced by tissue injury.

Although its precise cellular origin in biologic fluids and tissues has yet to be established, LPA production has been demonstrated in response to injury and has been shown to promote wound healing in multiple

tissues, including the skin (7,21,22). Recurrent tissue injury and aberrant wound healing responses appear to contribute to the pathogenesis of multiple fibrotic diseases, including scleroderma (1,23), and arachidonoyl (20:4) LPA levels were recently noted to be significantly higher in the serum of SSc patients as compared with healthy controls (6). We would therefore expect LPA levels to be increased in the skin during the development of injury-induced dermal fibrosis, both bleomycin-challenged mice and in SSc patients, although we have yet to investigate this.

Our initial investigations of the mechanism(s) through which LPA/LPA_1 signaling contributes to dermal fibrosis revealed that in contrast to WT mice, bleomycin-challenged LPA_1-KO mice failed to demonstrate two hallmarks of scleroderma-associated skin fibrosis: increased numbers of dermal myofibroblasts and increased numbers of dermal cells with nuclear Smad2 phosphorylation. These results suggest that LPA/LPA_1 signaling is required for two central processes in scleroderma fibrogenesis: myofibroblast accumulation and TGFβ/Smad signaling pathway activation. We believe that attenuation of both of these interconnected fibrogenic processes in the absence or inhibition of LPA_1 accounts for the dramatic protection of LPA_1-KO and AM095-treated mice from bleomycin-induced dermal fibrosis.

Myofibroblasts predominate in areas of increased collagen deposition in scleroderma lesional skin (24,25), where the number of myofibroblasts correlates with the severity of fibrosis (25). Promotion of myofibroblast accumulation by LPA/LPA_1 signaling would therefore be expected to promote dermal fibrosis. LPA mediates multiple fibroblast activities that lead to the accumulation of these cells, including their recruitment and proliferation, and the prevention of their apoptosis (3,22,26–31). We hypothesize that reduced fibroblast accumulation in the absence of LPA/LPA_1 signaling contributes to reduced myofibroblast accumulation in bleomycin-challenged LPA_1-KO mice by reducing the pool of cells from which myofibroblasts differentiate. Our ability to evaluate this hypothesis in our immunohistochemical studies, however, was limited by difficulties in enumerating tissue fibroblasts, as opposed to myofibroblasts, by immunostaining, due to the lack of antigens specifically expressed by these cells.

Evidence from both mouse models and SSc patients indicates that TGFβ plays a central role in scleroderma fibrogenesis. Fibroblast-specific expression of a constitutively active TGFβ receptor is sufficient to recapitulate many features of scleroderma in mice, including dermal fibrosis (32), while inhibition of TGFβ signaling protects against dermal fibrosis in commonly used mouse models of scleroderma, including the bleomycin model (33). Gene expression profiling of lesional skin from scleroderma patients demonstrates increased expression of many TGFβ targets, similar to gene expression induced by treating normal fibroblasts with TGFβ (10,34,35). In previous studies, we found that LPA_1 expression was not required for TGFβ downstream signaling in fibroblasts, since increases in procollagen type I α1 chain, fibronectin, and α-SMA expression induced by TGFβ were similar in WT and LPA_1-deficient mouse lung fibroblasts (3).

TGFβ activity, however, is primarily regulated through the posttranslational activation of latent TGFβ complexes (36,37). The failure of phospho-Smad2+ cells to increase in bleomycin-challenged LPA_1-KO mice therefore raises the possibility that LPA/LPA_1 signaling may mediate TGFβ *activation* during the development of dermal fibrosis. Although decreased fibroblast and myofibroblast accumulation in bleomycin-challenged LPA_1-KO mice could also have contributed to the reduced number of nuclear phospho-Smad2+ cells observed by decreasing the number of TGFβ-responsive cells present in the dermis, LPA has been reported to mediate TGFβ activation. LPA treatment of keratinocytes, as well as lung epithelial cells, has been shown to induce active TGFβ (4,38). While LPA signaling through LPA_2 has been shown to induce αvβ6 integrin–dependent activation of latent TGFβ by lung epithelial cells in culture (4), our results suggest that LPA_1 would be the receptor most likely to mediate LPA-induced TGFβ activation in the skin.

Activation of TGFβ by the epithelial cell-restricted αvβ6 integrin is required for the development of lung fibrosis in several animal models, including the bleomycin model of pulmonary fibrosis (5). In the lung, TGFβ-driven fibroblast activation and differentiation to myofibroblasts is therefore dependent on the activation of TGFβ by adjacent epithelial cells in a paracrine manner. In the skin of scleroderma patients however, activation of TGFβ by the fibroblasts themselves contributes to fibroblast activation and differentiation into myofibroblasts in an autocrine manner (39). The ability of scleroderma fibroblasts to activate TGFβ has been shown to result from their overexpression of 2 other αv-containing integrins that are capable of activating latent TGFβ, αvβ5 and αvβ3 (40,41). We therefore hypothesize that LPA signaling through LPA_1 mediates TGFβ activation during the development of dermal

fibrosis through the $\alpha v\beta 5$ and $\alpha v\beta 3$ integrins expressed by skin fibroblasts.

As noted above, our laboratory recently implicated LPA/LPA_1 signaling in the pathogenesis of pulmonary fibrosis (3). In addition, LPA has been implicated in renal and hepatic fibrogenesis. LPA_1-KO mice were shown to be significantly protected in the unilateral ureteral obstruction model of renal tubulointerstitial fibrosis (42), and concentrations of circulating LPA correlated with the extent of hepatic fibrosis in the carbon tetrachloride rodent model of liver fibrosis (43). Including our results in this study, data now implicate the LPA/LPA_1 pathway in the development of lung, kidney, liver, and skin fibrosis, suggesting that this pathway is of fundamental importance in the pathogenesis of fibrotic diseases associated with tissue injury. Additionally, the efficacy of a selective antagonist of LPA_1 in our dermal fibrosis model provides preclinical support for targeting LPA_1 in fibrotic diseases such as scleroderma.

In summary, we have shown that LPA signaling through LPA_1, but not LPA_2, is a critical requirement for the development of bleomycin-induced dermal fibrosis and for both myofibroblast accumulation and TGFβ/Smad signaling in this model. In addition to genetic deletion of LPA_1, we found that pharmacologic inhibition of this receptor in both preventive and therapeutic regimens protected mice from dermal fibrosis. The ability of AM095 to attenuate dermal fibrosis when initiated after the onset of tissue injury in a therapeutic regimen suggests that antagonism of LPA_1 may be effective in the treatment of patients with existing fibrosis, as would be needed for clinically useful antifibrotic drugs (40). Our results therefore indicate that LPA/LPA_1 inhibition has the potential to be an effective new therapeutic strategy for scleroderma and that LPA_1 is an attractive pharmacologic target for fibrosis.

ACKNOWLEDGMENT

The authors thank C. P. Leary for her expert assistance.

AUTHOR CONTRIBUTIONS

All authors were involved in drafting the article or revising it critically for important intellectual content, and all authors approved the final version to be published. Dr. Tager had full access to all of the data in the study and takes responsibility for the integrity of the data and the accuracy of the data analysis.

Study conception and design. Castelino, Seiders, Swaney, Lorrain, Chun, Luster, Tager.

Acquisition of data. Castelino, Bain, Brooks, King.

Analysis and interpretation of data. Castelino, Bain, King, Chun, Luster, Tager.

ROLE OF THE STUDY SPONSOR

Amira Pharmaceuticals facilitated the selectivity and pharmacokinetic studies of the LPA_1 receptor antagonist reported herein. They reviewed and approved the manuscript prior to submission. The authors independently collected the data, interpreted the results, and had the final decision to submit the manuscript for publication. Publication of this article was not contingent upon approval by Amira Pharmaceuticals.

REFERENCES

1. Abraham DJ, Varga J. Scleroderma: from cell and molecular mechanisms to disease models. Trends Immunol 2005;26:587–95.
2. Choi JW, Herr DR, Noguchi K, Yung YC, Lee CW, Mutoh T, et al. LPA receptors: subtypes and biological actions. Annu Rev Pharmacol Toxicol 2010;50:157–86.
3. Tager AM, Lacamera P, Shea BS, Campanella GS, Selman M, Zhao Z, et al. The lysophosphatidic acid receptor LPA_1 links pulmonary fibrosis to lung injury by mediating fibroblast recruitment and vascular leak. Nat Med 2008;14:45–54.
4. Xu MY, Porte J, Knox AJ, Weinreb PH, Maher TM, Violette SM, et al. Lysophosphatidic acid induces $\alpha v\beta 6$ integrin-mediated TGF-β activation via the LPA_2 receptor and the small G protein $G\alpha_q$. Am J Pathol 2009;174:1264–79.
5. Munger JS, Huang X, Kawakatsu H, Griffiths MJ, Dalton SL, Wu J, et al. A mechanism for regulating pulmonary inflammation and fibrosis: the integrin $\alpha v\beta 6$ binds and activates latent TGF $\beta 1$. Cell 1999;96:319–28.
6. Tokumura A, Carbone LD, Yoshioka Y, Morishige J, Kikuchi M, Postlethwaite A, et al. Elevated serum levels of arachidonoyl-lysophosphatidic acid and sphingosine 1-phosphate in systemic sclerosis. Int J Med Sci 2009;6:168–76.
7. Mazereeuw-Hautier J, Gres S, Fanguin M, Cariven C, Fauvel J, Perret B, et al. Production of lysophosphatidic acid in blister fluid: involvement of a lysophospholipase D activity. J Invest Dermatol 2005;125:421–7.
8. Yamamoto T, Takagawa S, Katayama I, Yamazaki K, Hamazaki Y, Shinkai H, et al. Animal model of sclerotic skin. I: Local injections of bleomycin induce sclerotic skin mimicking scleroderma. J Invest Dermatol 1999;112:456–62.
9. Wu M, Varga J. In perspective: murine models of scleroderma. Curr Rheumatol Rep 2008;10:173–82.
10. Whitfield ML, Finlay DR, Murray JI, Troyanskaya OG, Chi JT, Pergamenschikov A, et al. Systemic and cell type-specific gene expression patterns in scleroderma skin. Proc Natl Acad Sci U S A 2003;100:12319–24.
11. Takagawa S, Lakos G, Mori Y, Yamamoto T, Nishioka K, Varga J. Sustained activation of fibroblast transforming growth factor-β/Smad signaling in a murine model of scleroderma. J Invest Dermatol 2003;121:41–50.
12. Mori Y, Hinchcliff M, Wu M, Warner-Blankenship M, Lyons KM, Varga J. Connective tissue growth factor/CCN2-null mouse embryonic fibroblasts retain intact transforming growth factor-β responsiveness. Exp Cell Res 2008;314:1094–104.
13. Contos JJ, Fukushima N, Weiner JA, Kaushal D, Chun J. Requirement for the lp_{A1} lysophosphatidic acid receptor gene in normal suckling behavior. Proc Natl Acad Sci U S A 2000;97:13384–9.
14. Contos JJ, Ishii I, Fukushima N, Kingsbury MA, Ye X, Kawamura S, et al. Characterization of lpa_2 (Edg4) and lpa_1/lpa_2 (Edg2/Edg4) lysophosphatidic acid receptor knockout mice: signaling deficits without obvious phenotypic abnormality attributable to lpa_2. Mol Cell Biol 2002;22:6921–9.
15. Tager AM, Kradin RL, LaCamera P, Bercury SD, Campanella GS, Leary CP, et al. Inhibition of pulmonary fibrosis by the chemokine IP-10/CXCL10. Am J Respir Cell Mol Biol 2004;31:395–404.
16. Desmouliere A, Chaponnier C, Gabbiani G. Tissue repair, con-

traction, and the myofibroblast. Wound Repair Regen 2005;13: 7–12.
17. Abraham DJ, Eckes B, Rajkumar V, Krieg T. New developments in fibroblast and myofibroblast biology: implications for fibrosis and scleroderma. Curr Rheumatol Rep 2007;9:136–43.
18. Hinz B. Formation and function of the myofibroblast during tissue repair. J Invest Dermatol 2007;127:526–37.
19. Werner S, Grose R. Regulation of wound healing by growth factors and cytokines. Physiol Rev 2003;83:835–70.
20. Massague J, Seoane J, Wotton D. Smad transcription factors. Genes Dev 2005;19:2783–810.
21. Demoyer JS, Skalak TC, Durieux ME. Lysophosphatidic acid enhances healing of acute cutaneous wounds in the mouse. Wound Repair Regen 2000;8:530–7.
22. Balazs L, Okolicany J, Ferrebee M, Tolley B, Tigyi G. Topical application of the phospholipid growth factor lysophosphatidic acid promotes wound healing in vivo. Am J Physiol Regul Integr Comp Physiol 2001;280:R466–72.
23. Abraham D, Distler O. How does endothelial cell injury start? The role of endothelin in systemic sclerosis. Arthritis Res Ther 2007;9 Suppl 2:S2.
24. Sappino AP, Masouye I, Saurat JH, Gabbiani G. Smooth muscle differentiation in scleroderma fibroblastic cells. Am J Pathol 1990;137:585–91.
25. Kissin EY, Merkel PA, Lafyatis R. Myofibroblasts and hyalinized collagen as markers of skin disease in systemic sclerosis. Arthritis Rheum 2006;54:3655–60.
26. Kundra V, Anand-Apte B, Feig LA, Zetter BR. The chemotactic response to PDGF-BB: evidence of a role for Ras. J Cell Biol 1995;130:725–31.
27. Pietruck F, Busch S, Virchow S, Brockmeyer N, Siffert W. Signalling properties of lysophosphatidic acid in primary human skin fibroblasts: role of pertussis toxin-sensitive GTP-binding proteins. Naunyn Schmiedebergs Arch Pharmacol 1997;355:1–7.
28. Cerutis DR, Dreyer A, Cordini F, McVaney TP, Mattson JS, Parrish LC, et al. Lysophosphatidic acid modulates the regenerative responses of human gingival fibroblasts and enhances the actions of platelet-derived growth factor. J Periodontol 2004;75: 297–305.
29. Tangkijvanich P, Melton AC, Chitapanarux T, Han J, Yee HF. Platelet-derived growth factor-BB and lysophosphatidic acid distinctly regulate hepatic myofibroblast migration through focal adhesion kinase. Exp Cell Res 2002;281:140–7.
30. Fang X, Yu S, LaPushin R, Lu Y, Furui T, Penn LZ, et al. Lysophosphatidic acid prevents apoptosis in fibroblasts via G_i-protein-mediated activation of mitogen-activated protein kinase. Biochem J 2000;352 Pt 1:135–43.
31. Song J, Clair T, Noh JH, Eun JW, Ryu SY, Lee SN, et al. Autotaxin (lysoPLD/NPP2) protects fibroblasts from apoptosis through its enzymatic product, lysophosphatidic acid, utilizing albumin-bound substrate. Biochem Biophys Res Commun 2005; 337:967–75.
32. Sonnylal S, Denton CP, Zheng B, Keene DR, He R, Adams HP, et al. Postnatal induction of transforming growth factor β signaling in fibroblasts of mice recapitulates clinical, histologic, and biochemical features of scleroderma. Arthritis Rheum 2007;56: 334–44.
33. Lakos G, Takagawa S, Chen SJ, Ferreira AM, Han G, Masuda K, et al. Targeted disruption of TGF-β/Smad3 signaling modulates skin fibrosis in a mouse model of scleroderma. Am J Pathol 2004;165:203–17.
34. Gardner H, Shearstone JR, Bandaru R, Crowell T, Lynes M, Trojanowska M, et al. Gene profiling of scleroderma skin reveals robust signatures of disease that are imperfectly reflected in the transcript profiles of explanted fibroblasts. Arthritis Rheum 2006; 54:1961–73.
35. Milano A, Pendergrass SA, Sargent JL, George LK, McCalmont TH, Connolly MK, et al. Molecular subsets in the gene expression signatures of scleroderma skin. PLoS One 2008;3:e2696.
36. Munger JS, Harpel JG, Gleizes PE, Mazzieri R, Nunes I, Rifkin DB. Latent transforming growth factor-β: structural features and mechanisms of activation. Kidney Int 1997;51:1376–82.
37. Annes JP, Munger JS, Rifkin DB. Making sense of latent TGFβ activation. J Cell Sci 2003;116:217–24.
38. Piazza GA, Ritter JL, Baracka CA. Lysophosphatidic acid induction of transforming growth factors α and β: modulation of proliferation and differentiation in cultured human keratinocytes and mouse skin. Exp Cell Res 1995;216:51–64.
39. Ihn H, Yamane K, Kubo M, Tamaki K. Blockade of endogenous transforming growth factor β signaling prevents up-regulated collagen synthesis in scleroderma fibroblasts: association with increased expression of transforming growth factor β receptors. Arthritis Rheum 2001;44:474–80.
40. Asano Y, Ihn H, Yamane K, Kubo M, Tamaki K. Increased expression levels of integrin $\alpha v\beta 5$ on scleroderma fibroblasts. Am J Pathol 2004;164:1275–92.
41. Asano Y, Ihn H, Yamane K, Jinnin M, Mimura Y, Tamaki K. Increased expression of integrin $\alpha_v\beta_3$ contributes to the establishment of autocrine TGF-β signaling in scleroderma fibroblasts. J Immunol 2005;175:7708–18.
42. Pradere JP, Klein J, Gres S, Guigne C, Neau E, Valet P, et al. LPA_1 receptor activation promotes renal interstitial fibrosis. J Am Soc Nephrol 2007;18:3110–8.
43. Watanabe N, Ikeda H, Nakamura K, Ohkawa R, Kume Y, Tomiya T, et al. Plasma lysophosphatidic acid level and serum autotaxin activity are increased in liver injury in rats in relation to its severity. Life Sci 2007;81:1009–15.